CDF note 9157

Measurement of the $t\bar{t}$ differential cross section, $d\sigma/dM_{t\bar{t}}$

The CDF Collaboration
URL http://www-cdf.fnal.gov
(Dated: January 9, 2008)

We present a measurement of the $t\bar{t}$ differential cross section, $d\sigma/dM_{t\bar{t}}$, at $\sqrt{s} = 1.96$ TeV using $\sim 1.9\ fb^{-1}$ of data collected with the CDF II Detector at the Fermilab Tevatron. We select events in the $W+ \geq 4$ jets sample with displaced secondary vertices from jets with heavy-flavor decays. We use a regularized unfolding technique to correct the reconstructed invariant mass distribution back to the true distribution. We see no evidence of inconsistency with the Standard Model, with an observed p-value of 0.45.

Preliminary Results for Winter 2008 Conferences

I. INTRODUCTION

The top quark, the most massive of the elementary particles, is the only known particle which has mass on the order of the electroweak symmetry breaking (EWSB) scale. For this reason, the top quark plays a special role in many beyond the Standard Model (BSM) theories of EWSB. In these theories, new gauge interactions produce massive particles which may couple strongly to the top quark. Such particles may produce resonances in the invariant mass distribution of the top quark via a $p\overline{p} \to X \to t\overline{t}$ process, or may interfere with the Standard Model (SM) process and cause distortions to the shape of the invariant mass distribution. [1]

We measure $d\sigma/dM_{t\overline{t}}$, as defined by:

$$\frac{d\sigma^i}{dM_{t\overline{t}}} = \frac{N_i - N_i^{bkg}}{\mathcal{A}_i \int \mathcal{L} \Delta^i_{M_{t\overline{t}}}}$$

where N_i is the number of events, N_i^{bkg} is the predicted number of background events and $\mathcal{A}_i$ is the acceptance in bin i; $\Delta^i_{M_{t\overline{t}}}$ is the width of bin i; and $\int \mathcal{L}$ is the integrated luminosity. We divide the $M_{t\overline{t}}$ distribution into 8 bins – 0-350, 350-400, 400-450, 450-500, 500-550, 550-600, 600-700 and 700-1400 GeV/c^2. We check for consistency with the SM by comparing a test statistic to a distribution generated from Monte Carlo experiments.

II. DATA SAMPLE & EVENT SELECTION

We use $\sim 1.9\ fb^{-1}$ of CDF II data, collected between March 2002 and May 2007. The data are collected with an inclusive lepton trigger, which requires an electron or muon with E_T or $p_T >$ 18 GeV/c. The offline selection requires a lepton with $E_T > 20\ GeV$ ($p_T > 20\ GeV/c$ for muons), missing transverse energy greater than 20 GeV and at least 4 jets with $E_T > 20\ GeV$. To further reduce the backgrounds, we require at least one jet with an identified displaced secondary vertex, from a heavy-flavor decay. We identify these jets as b-jets ("b-tagged") from the decay $t \to Wb$. With this event selection, we observe 484 total events. The CDF II detector is described in detail elsewhere [2].

We reconstruct the invariant mass of the $t\overline{t}$ pair by combining the 4-vectors the of the 4 leading jets, lepton and missing transverse energy. This reconstructed $M_{t\overline{t}}$ distribution is distorted from the true distribution by detector effects, including jet and missing energy resolution, and our geometric and kinematic acceptance. We correct for these effects by using a regularized unfolding technique, Singular Value Decomposition (SVD) unfolding [4].

A. Acceptance

The total $t\overline{t}$ acceptance is measured from a mixture of data and Monte Carlo. We use a `PYTHIA` Monte Carlo simulation [3] to measure the geometric and kinematic acceptance. The efficiency is measured in data using the unbiased leg of $Z \to \ell\ell$ decays. The difference in efficiency for identifying an isolated high p_T lepton in data versus Monte Carlo is corrected for with a scale factor. Likewise we correct for the difference in data and Monte Carlo for tagging a b-jet. The efficiency in data is determined in a heavy-flavor enriched data sample of low p_T electrons, from the semi-leptonic decay of B hadrons and mesons. The total acceptance in each bin, including these scale factors and the efficiencies of the trigger, times the integrated luminosity is given in Table I.

B. SVD Data Unfolding

In order to extract the true underlying $M_{t\overline{t}}$ distribution from the reconstructed distribution, it is possible to model the effects which distort $M_{t\overline{t}}$ with Monte Carlo and produce a probability response

CDF II Preliminary, $\int \mathcal{L} = 1.9 \pm 0.1\ fb^{-1}$				
$M_{t\bar{t}}$ $[GeV/c^2]$	CEM	CMUP	CMX	All Leptons
Denominator without bin width $[pb^{-1}]$				
≤ 350	16.98 ± 1.10	10.21 ± 0.65	4.55 ± 0.29	31.74 ± 1.31
350-400	25.33 ± 1.63	13.93 ± 0.89	6.63 ± 0.42	45.89 ± 1.91
400-450	28.39 ± 1.83	15.64 ± 1.00	7.27 ± 0.46	51.29 ± 2.14
450-500	29.80 ± 1.92	16.70 ± 1.07	7.48 ± 0.48	53.97 ± 2.25
500-550	31.37 ± 2.02	17.57 ± 1.12	8.11 ± 0.52	57.05 ± 2.37
550-600	32.07 ± 2.07	17.97 ± 1.15	8.03 ± 0.51	58.08 ± 2.42
600-700	32.27 ± 2.08	17.75 ± 1.13	8.49 ± 0.54	58.52 ± 2.43
700-1400	30.78 ± 1.99	16.05 ± 1.02	7.46 ± 0.48	54.30 ± 2.28
All bins	28.12 ± 1.81	15.57 ± 0.99	7.23 ± 0.46	50.92 ± 2.12
Assumes $M_{top} = 175\ GeV/c^2$				

TABLE I: The values of the denominator of $d\sigma/dM_{t\bar{t}}$ in each bin, excluding the multiplication by bin width.

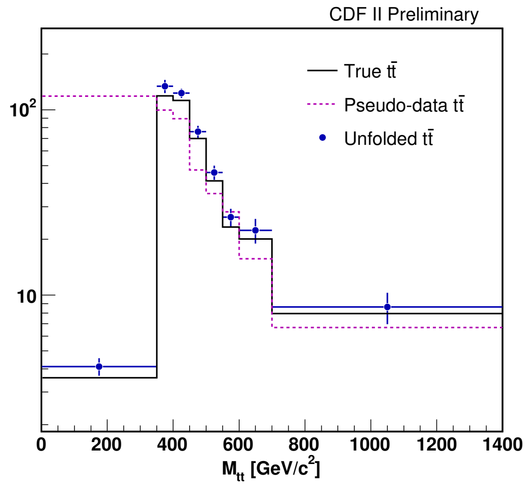

FIG. 1: An example unfolded $M_{t\bar{t}}$ distribution compared with the true and a simulated measured distribution.

matrix, $\hat{A}$, such that $\hat{A}x = b$ where x is the true distribution and b is the measured distribution. However, given the measured distribution b, attempting to solve for x by inverting $\hat{A}$ results in solutions with large differences from the true distribution when some bins are not well populated. We use the technique described in [4], which uses the SVD of a response matrix filled with actual numbers of events, rather than probabilities, to regularize the solution. Figure 1 shows an application of the algorithm to a simulated reconstructed distribution of events.

III. BACKGROUNDS

The $t\bar{t}$ signature described in Section II can be mimicked by several Standard Model processes, including diboson production, single top production, and W+jets production. The least-well theoretically constrained of these processes is the W+jets production cross section, due to the difficulties of high-order QCD calculations. We use a background estimation, described previously in [5], which uses the theoretically well-known processes to constrain the data sample composition.

The calculation of the expected number of events from the electroweak processes – diboson, Z+jets, single top – is straightforward. We calculate an acceptance for each process, analogously to the $t\bar{t}$ acceptance described in Section II A, and obtain the total number of expected events according to $N = \sigma\mathcal{A}\int\mathcal{L}$. These processes, with the exception of single-top and Z+jets, are modeled with a PYTHIA Monte Carlo simulation. The single-top background is modeled by a MADEVENT [6] Monte Carlo simulation which is showered with PYTHIA, the Z+jets background is modeled by an ALPGEN [7] Monte Carlo simulation which is showered by PYTHIA. These backgrounds are small for our event selection.

The largest component of the background is W+jets production. We separate the tagged heavy flavor component of the W+jets background from the tagged light flavor component. We assume that while the absolute cross section for heavy flavor production is very sensitive to higher order corrections, that the fraction is not. Therefore we calculate the fraction of W+jets events with bottom and charm content in an ALPGEN Monte Carlo simulation with PYTHIA showering, and obtain the absolute normalization from the number of W+jets events before the tagging selection ("pretag") in the data. The number of pretag W+jets events is equal to the number of events from electroweak processes, QCD events with no real W, and $t\bar{t}$ production subtracted from the number of events observed at pretag. The number of expected W+heavy flavor events we obtain is corrected for differences in heavy flavor content and tagging efficiency in data and Monte Carlo.

The QCD background expectation is obtained by fitting the shape of the missing E_T distribution in data. Events with no real W will generally have low missing energy because of the absence of a high p_T neutrino. The fit allows an extrapolation from the low missing energy side band to the signal region, with missing E_T greater than 20 GeV.

The remainder of the W+jets background in the tagged data is a result of the misidentification of light flavor jets as heavy flavor, or "mistags". To first order, the mistags may be modeled by events with negative tags, which occur when the secondary vertex is reconstructed behind the interaction point. The rate of negative tags is parameterized as a function of jet energy, jet η, number of tracks, number of z-vertices, primary vertex position and the sum of the event transverse energy in a mistag matrix. The sum of probabilities from the matrix on all jets in the event yields the number of negative tags. This number is corrected for an asymmetry in the negative versus positive decay probability for mistags and real heavy flavor content of the mistag matrix. The predicted number of W+light flavor events is then the number of negative tags times the fraction of W+light flavor events in the W+jets sample.

The composition of our data sample is summarized in Table II.

CDF II Preliminary, $\int\mathcal{L} = 1.9 \pm 0.1\ fb^{-1}$	
Process	Prediction
$Wbb/Wcc/Wc$	35.5 $\pm$ 14.06
Mistags	19.9 $\pm$ 4.73
non-W	18.2 $\pm$ 16.29
Single Top	4.7 $\pm$ 0.44
Other electroweak	7.4 $\pm$ 0.79
Total Background Prediction	85.7 $\pm$ 22.0
Observed	484
Measured $t\bar{t}$	398.3 $\pm$ 22.0

TABLE II: Summary of sample composition.

IV. SYSTEMATIC UNCERTAINTIES

Our systematic uncertainties arise from Monte Carlo modeling of the acceptance, true and reconstructed $M_{t\bar{t}}$ distributions, and background distributions; also, the uncertainties of our efficiency of lepton identification, b-tagging efficiency, and integrated luminosity affect the measurement. The lepton identification uncertainty arises due to the extrapolation from $Z \to \ell\ell$ events, where the efficiency is measured in data, to the busier $t\bar{t}$ environment. The uncertainty on the b-tagging efficiency is largely dominated by the limited number of events in the data sample that is used. These uncertainties, along with the uncertainty due to the size of the Monte Carlo sample used to determine the geometric and kinematic acceptance in each bin, comprise the total acceptance uncertainty in Table III.

We evaluate the effect of the remaining uncertainties by performing large sets of pseudo-experiments, where we create a pseudo-data distribution, based upon Monte Carlo modeling of the sample composition, fluctuate that distribution and then measure the differential cross section. To test the effect of changing, for example, the Monte Carlo generator, we create a pseudo-data distribution where the $t\bar{t}$ signal is modeled by a `HERWIG` [8] Monte Carlo simulation and compare the mean measured $d\sigma/dM_{t\bar{t}}$ in each bin in many pseudo-experiments to the mean using our default generator. The difference in the mean $d\sigma/dM_{t\bar{t}}$ is taken as the systematic uncertainty. The systematic uncertainty due to the amount of initial and final state radiation, jet energy scale, and parton distribution function are evaluated in an analogous manner – we add more or less ISR or FSR to the signal, shift the jet energy scale, or change the PDF and take as an uncertainty the difference in the mean measured $d\sigma/dM_{t\bar{t}}$ in pseudo-experiments. To assess the uncertainty due to our modeling of the background we vary both the overall normalization of the background, according to the uncertainty on the prediction as given in Table II, and the shape of the background in the pseudo-data. Again the difference in the mean measured $d\sigma/dM_{t\bar{t}}$ is taken as the uncertainty. These results are all summarized in Table III.

Overall, the uncertainties due to jet energy scale, Monte Carlo generator, background modeling and parton distribution function dominate. The uncertainties are smallest near the threshold for $t\bar{t}$ prediction (14.1-16.1%) and largest in the tails of the distribution (21.4-40.2%).

Summary of systematic uncertainties for $d\sigma/dM_{t\bar{t}}$ measurement CDF II Preliminary, $\int \mathcal{L} = 1.9 \pm 0.1\ fb^{-1}$								
$M_{t\bar{t}}$ $[GeV/c^2]$	0-350	350-400	400-450	450-500	500-550	550-600	600-700	700-1400
MC Generator [%]	13.6	10.0	2.8	4.9	10.9	15.7	19.6	22.1
Initial State Radiation [%]	8.7	5.8	1.2	4.5	6.7	6.9	6.4	6.1
Final State Radiation [%]	4.6	3.1	0.7	2.1	2.9	3.0	3.7	4.7
Jet Energy Scale [%]	16.0	11.0	2.1	7.9	12.9	15.8	17.9	19.3
Background Shape [%]	30.2	24.6	14.1	7.8	6.8	9.0	12.1	14.3
Background Normalization [%]	9.4	7.7	4.6	2.9	3.0	4.0	5.3	6.1
Acceptance [%]	4.1	4.2	4.2	4.2	4.2	4.2	4.2	4.2
MC PDF Set [%]	7.9	6.3	3.0	1.6	6.9	12.6	17.5	20.6
Total [%]	40.2	31.4	16.1	14.1	21.4	28.7	35.5	40.0

TABLE III: Summary of systematic uncertainties in each bin. The 6% uncertainty due to luminosity is not included in the total.

V. RESULTS

The $M_{t\bar{t}}$ distribution we reconstruct in data is shown in Figure 2. The unfolded background-subtracted distribution is shown in Figure 3. To derive $d\sigma/dM_{t\bar{t}}$, we divide the contents of each bin of the unfolded distribution by the appropriate denominator in Table I. The result is shown in Figure 4 and also presented in Table IV.

We check consistency with the Standard Model measurement using the Anderson-Darling statistic [9]. This statistic is similar to the more commonly used Kolmogorov-Smirnov statistic, but it puts more emphasis on discrepancies in the tail of the distribution. We omit the first bin of the distribution ($M_{t\bar{t}} < 350$ GeV), when calculating this statistic. The Anderson-Darling statistic distribution in pseudo-experiments, and the observed value in the data are presented in Figure 5.

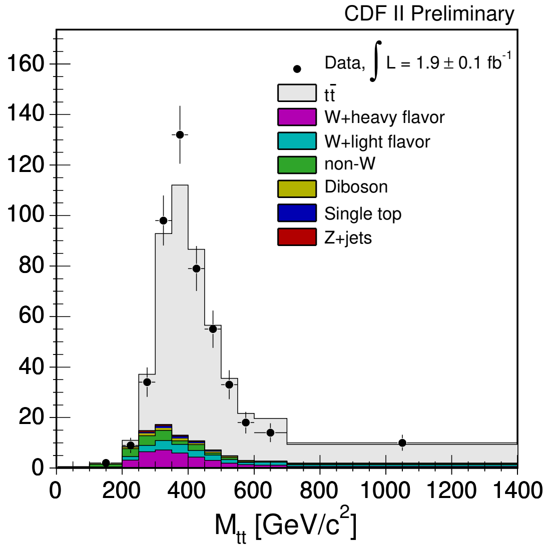

FIG. 2: Reconstructed $M_{t\bar{t}}$ distribution in 1.9 fb^{-1} of $W+\geq 4$ jets data. The first five bins ($M_{t\bar{t}} \leq 350$ GeV) are combined for the $d\sigma/dM_{t\bar{t}}$ measurement.

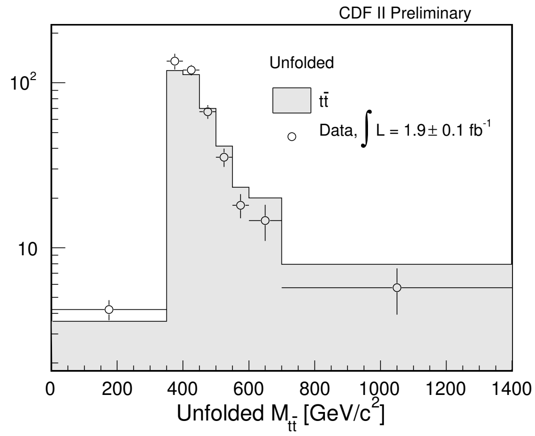

FIG. 3: Unfolded $M_{t\bar{t}}$ distribution in 1.9 fb^{-1} of $W+\geq 4$ jets data. The $t\bar{t}$ expectation is for a total $t\bar{t}$ cross section of 7.8 pb.

We calculate a p-value by taking the fraction of experiments in pseudo-experiments with a larger observed Anderson-Darling statistic than that in data. The observed p-value is 0.45.

As a cross check we repeat the measurement using only events with tight electrons or tight muons. The results are presented in Tables V and VI, respectively. There is no significant discrepancy between the measurements.

We also perform the measurement with the higher purity double-tagged sample. The reconstructed and unfolded distributions in the double-tagged sample are shown in Figures 6 and 7, respectively. The measurement is presented in Table VII. The final result, with systematic uncertainties included, is presented in Table VIII. For top quark mass of 170 GeV/c^2, the differences in $d\sigma/dM_{t\bar{t}}$ are insignificant, except in the first bin ($M_{top} \leq 350$ GeV/c^2). The measured value in that bin is 0.0013 ± 0.002 pb/GeV/c^2 (stat. uncertainties only).

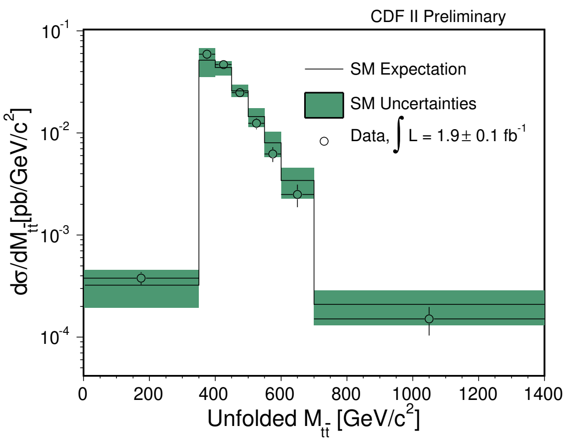

FIG. 4: $d\sigma/dM_{t\bar{t}}$ in 1.9 fb^{-1} of $W+\geq 4$ jets data. The $t\bar{t}$ expectation is for a total $t\bar{t}$ cross section of 7.8 pb.

$W \to \ell\nu + \geq 4$ jets data with ≥ 1 secondary vertex tag CDF II Preliminary, $\int \mathcal{L} = 1.9 \pm 0.1\ fb^{-1}$		
$M_{t\bar{t}}$ $[GeV/c^2]$	$N_{t\bar{t}}^{unfolded}$	$d\sigma/dM_{t\bar{t}}$ $[pb/GeV/c^2]$ (stat. uncertainties only)
$\leq$ 350	4.21 ± 0.59	0.00038 ± 5.3e-05
350-400	135.27 ± 14.69	0.059 ± 0.0064
400-450	119.63 ± 8.69	0.047 ± 0.0034
450-500	66.90 ± 6.45	0.025 ± 0.0024
500-550	35.42 ± 4.50	0.012 ± 0.0016
550-600	18.10 ± 3.03	0.0062 ± 0.001
600-700	14.61 ± 3.62	0.0025 ± 0.00062
700-1400	5.72 ± 1.79	0.00015 ± 4.7e-05
Assumes $M_{top} = 175\ GeV/c^2$		

TABLE IV: The unfolded number of $t\bar{t}$ events and differential cross section in each bin.

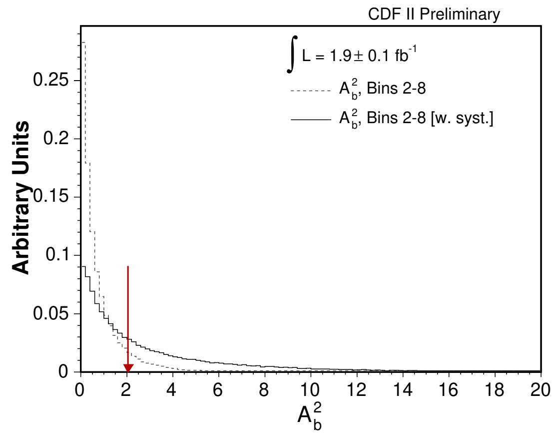

FIG. 5: Distribution of Anderson-Darling statistic in pseudo-experiments. The value observed in data – 2.09 – is indicated by the red arrow.

$W \to e\nu + \geq 4$ jets data with ≥ 1 secondary vertex tag CDF II Preliminary, $\int \mathcal{L} = 1.9 \pm 0.1\ fb^{-1}$		
$M_{t\bar{t}}$ $[GeV/c^2]$	$N_{t\bar{t}}^{unfolded}$	$d\sigma/dM_{t\bar{t}}$ $[pb/GeV/c^2]$ (stat. uncertainties only)
≤ 350	2.27 $\pm$ 0.44	0.00038 $\pm$ 7.3e-05
350-400	74.21 $\pm$ 11.26	0.059 $\pm$ 0.0089
400-450	64.08 $\pm$ 6.60	0.045 $\pm$ 0.0047
450-500	35.48 $\pm$ 4.84	0.024 $\pm$ 0.0032
500-550	19.96 $\pm$ 3.42	0.013 $\pm$ 0.0022
550-600	11.34 $\pm$ 2.36	0.0071 $\pm$ 0.0015
600-700	10.04 $\pm$ 2.83	0.0031 $\pm$ 0.00088
700-1400	4.20 $\pm$ 1.42	0.00019 $\pm$ 6.6e-05
Assumes $M_{top} = 175\ GeV/c^2$		

TABLE V: A cross check, using only data with electrons.

$W \to \mu\nu + \geq 4$ jets data with ≥ 1 secondary vertex tag CDF II Preliminary, $\int \mathcal{L} = 1.9 \pm 0.1\ fb^{-1}$		
$M_{t\bar{t}}$ $[GeV/c^2]$	$N_{t\bar{t}}^{unfolded}$	$d\sigma/dM_{t\bar{t}}$ $[pb/GeV/c^2]$ (stat. uncertainties only)
≤ 350	1.97 $\pm$ 0.39	0.00038 $\pm$ 7.5e-05
350-400	61.13 $\pm$ 9.36	0.059 $\pm$ 0.0091
400-450	54.94 $\pm$ 5.64	0.048 $\pm$ 0.0049
450-500	30.75 $\pm$ 4.22	0.025 $\pm$ 0.0035
500-550	15.09 $\pm$ 2.89	0.012 $\pm$ 0.0022
550-600	6.53 $\pm$ 1.88	0.005 $\pm$ 0.0014
600-700	4.45 $\pm$ 2.25	0.0017 $\pm$ 0.00086
700-1400	1.54 $\pm$ 1.07	9.4e-05 $\pm$ 6.5e-05
Assumes $M_{top} = 175\ GeV/c^2$		

TABLE VI: A cross check, using only data with muons.

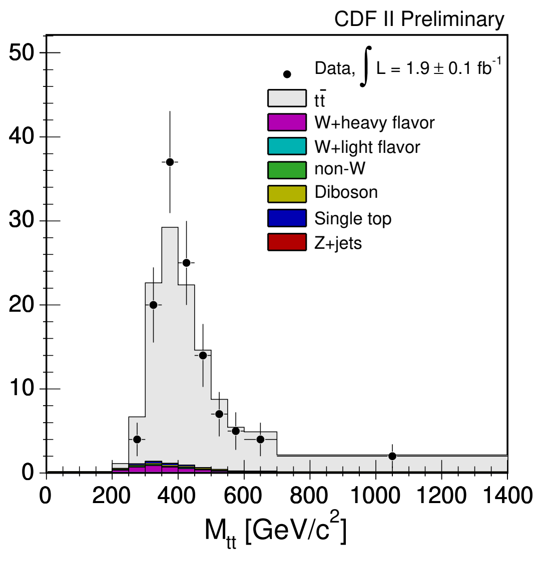

FIG. 6: Reconstructed $M_{t\bar{t}}$ distribution in 1.9 fb^{-1} of double-tagged $W+\geq 4$ jets data.

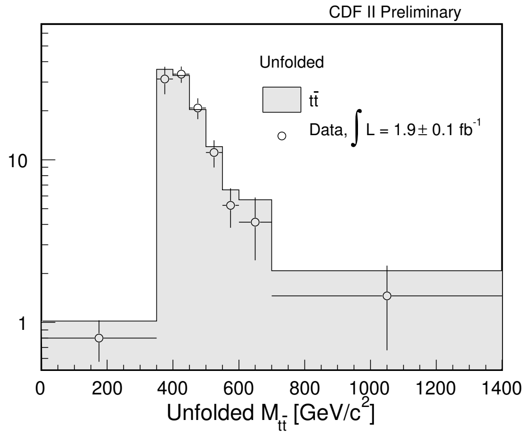

FIG. 7: Unfolded $M_{t\bar{t}}$ distribution in 1.9 fb^{-1} of double-tagged $W+\geq$ 4 jets data.

$W \rightarrow \ell\nu+ \geq 4$ jets data with ≥ 2 secondary vertex tags CDF II Preliminary, $\int \mathcal{L} = 1.9 \pm 0.1\ fb^{-1}$		
$M_{t\bar{t}}$ $[GeV/c^2]$	$N_{t\bar{t}}^{unfolded}$	$d\sigma/dM_{t\bar{t}}$ $[pb/GeV/c^2]$ (stat. uncertainties only)
$\leq$ 350	0.80 ± 0.23	0.00026 ± 7.3e-05
350-400	31.33 ± 6.02	0.045 ± 0.0086
400-450	33.57 ± 3.85	0.045 ± 0.0051
450-500	20.84 ± 3.06	0.027 ± 0.0039
500-550	11.08 ± 2.12	0.013 ± 0.0025
550-600	5.24 ± 1.42	0.0064 ± 0.0017
600-700	4.13 ± 1.72	0.0025 ± 0.001
700-1400	1.45 ± 0.78	0.00014 ± 7.8e-05
Assumes $M_{top} = 175\ GeV/c^2$		

TABLE VII: A cross check, using the higher purity double-tag sample.

VI. CONCLUSIONS

Using a sample of 484 total events in 1.9 fb^{-1} of CDF II data, of which the expected background total is 85.7 ± 22.0, we have measured the $t\bar{t}$ differential cross section, $d\sigma/dM_{t\bar{t}}$. The shape of the differential cross section is sensitive to potential sources of new physics that could appear as resonances, broad enhancements, or interference effects in the $M_{t\bar{t}}$ distribution. We use an Anderson-Darling statistic to test for such discrepancies from the Standard Model expectation. None are found. Our measurement is consistent with the Standard Model with a p-value of 0.45

$W \to \ell\nu + \geq 4$ jets data with ≥ 1 secondary vertex tags CDF II Preliminary, $\int \mathcal{L} = 1.9 \pm 0.1\ fb^{-1}$	
$M_{t\bar{t}}$ $[GeV/c^2]$	$d\sigma/dM_{t\bar{t}}$ $[pb/GeV/c^2]$
≤ 350	0.00038 $\pm$ 5.3e-05 (stat.) $\pm$ 0.00015 (syst.) $\pm$ 2.3e-05 (lumi.)
350-400	0.059 $\pm$ 0.0064 (stat.) $\pm$ 0.018 (syst.) $\pm$ 0.0035 (lumi.)
400-450	0.047 $\pm$ 0.0034 (stat.) $\pm$ 0.0075 (syst.) $\pm$ 0.0028 (lumi.)
450-500	0.025 $\pm$ 0.0024 (stat.) $\pm$ 0.0035 (syst.) $\pm$ 0.0015 (lumi.)
500-550	0.012 $\pm$ 0.0016 (stat.) $\pm$ 0.0027 (syst.) $\pm$ 0.00075 (lumi.)
550-600	0.0062 $\pm$ 0.001 (stat.) $\pm$ 0.0018 (syst.) $\pm$ 0.00037 (lumi.)
600-700	0.0025 $\pm$ 0.00062 (stat.) $\pm$ 0.00089 (syst.) $\pm$ 0.00015 (lumi.)
700-1400	0.00015 $\pm$ 4.7e-05 (stat.) $\pm$ 6e-05 (syst.) $\pm$ 9e-06 (lumi.)
Assumes $M_{top} = 175\ GeV/c^2$	

TABLE VIII: The measured $d\sigma/dM_{t\bar{t}}$ in each bin, with all uncertainties.

Acknowledgments

We thank the Fermilab staff and the technical staffs of the participating institutions for their vital contributions. This work was supported by the U.S. Department of Energy and National Science Foundation; the Italian Istituto Nazionale di Fisica Nucleare; the Ministry of Education, Culture, Sports, Science and Technology of Japan; the Natural Sciences and Engineering Research Council of Canada; the National Science Council of the Republic of China; the Swiss National Science Foundation; the A.P. Sloan Foundation; the Bundesministerium für Bildung und Forschung, Germany; the Korean Science and Engineering Foundation and the Korean Research Foundation; the Science and Technology Facilities Council and the Royal Society, UK; the Institut National de Physique Nucleaire et Physique des Particules/CNRS; the Russian Foundation for Basic Research; the Comisión Interministerial de Ciencia y Tecnología, Spain; the European Community's Human Potential Programme; the Slovak R&D Agency; and the Academy of Finland.

---

[1] Christopher T. Hill and Stephen J. Parke, Phys. Rev. D **49**, 4454 (1994); D. Dicus, A. Stange, S. Willenbrock, Phys. Lett. B; G. Cvetic, Reviews of Modern Physics **71**, 513(1999); R. Frederix and F. Maltoni."Top pair invariant mass distribution: a window on new physics." (2007)hep-ph/0712.2355v1.

[2] F. Abe, et al., Nucl. Instrum. Methods Phys. Res. A **271**, 387 (1988); D. Amidei, et al., Nucl. Instum. Methods Phys. Res. A **350**, 73 (1994); F. Abe, et al., Phys. Rev. D **52**, 4784 (1995); P. Azzi, et al., Nucl. Instrum. Methods Phys. Res. A **360**, 137 (1995); The CDFII Detector Technical Design Report, Fermilab-Pub-96/390-E.

[3] T. Sjostrand et al., High-Energy-Physics Event Generation with PYTHIA 6.1, Comput. Phys. Commun. **135**, 238 (2001).

[4] A. Hocker and V. Kartvelishivili. "SVD Approach to Data Unfolding." (1995)hep-ph/9509307.

[5] CDF Public Note 8795. "Measurement of the $t\bar{t}$ Production Cross Section in $p\bar{p}$ collisions at $\sqrt{s}$ = 1.96 TeV using Lepton+Jets Events with Secondary Vertex b-tagging; A. Abulencia, et al., Phys. Rev. Lett. **97**, 082004 (2006).

[6] F. Maltoni and T. Stelzer, JHEP **0302**, 027 (2003).

[7] M. L. Mangano, et al., JHEP **07**,1 (2003).

[8] G. Corcella et al., HERWIG 6: An Event Generator for Hadron Emission Reactions with Interfering Gluons (including supersymmetric processes), JHEP **01**, 10 (2001).

[9] T. W. Anderson and D. A. Darling, The Annals of Mathematical Statistics **23**, 193 (1952).